ACS APPLIED MATERIALS & INTERFACES

Research Article

www.acsami.org

Ultrastable and Atomically Smooth Ultrathin Silver Films Grown on a Copper Seed Layer

Nadia Formica,*[,†,⊥] Dhriti S. Ghosh,[†,⊥] Albert Carrilero,[†] Tong Lai Chen,[†] Robert E. Simpson,[§] and Valerio Pruneri[†,‡]

[†]ICFO-Institut de Ciències Fotòniques, Mediterranean Technology Park, Castelldefels, Barcelona, 08860 Spain

[‡]ICREA-Institució Catalana de Recerca i Estudis Avancats, Barcelona, 08010 Spain

[§]Singapore University of Technology and Design, 20 Dover Drive, Singapore

ABSTRACT: An effective method to deposit atomically smooth ultrathin silver (Ag) films by employing a 1 nm copper (Cu) seed layer is reported. The inclusion of the Cu seed layer leads to the deposition of films with extremely low surface roughness (<0.5 nm), while it also reduces the minimum thickness required to obtain a continuous Ag film (percolation thickness) to 3 nm compared to 6 nm without the seed layer. Moreover, the Cu seed layer alters the growth mechanism of the Ag film by providing energetically favorable nucleation sites for the incoming Ag atoms leading to an improved surface morphology and concomitant lower electrical sheet resistance. Optical measurements together with X-ray diffraction and electrical resistivity measurements confirmed that the Ag film undergoes a layer-by-layer growth mode resulting in a smaller grain size. The Cu seeded Ag growth method provides a feasible way to deposit ultrathin Ag films for nanoscale electronic, plasmonic and photonic applications. In addition, as a result of the improved uniformity, the oxidation of the Ag layer is strongly reduced to negligible values.

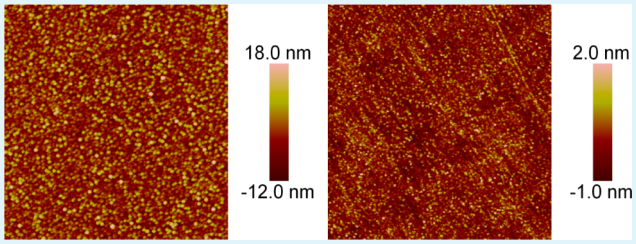

KEYWORDS: *silver, seed layer, ultrathin, ultrasmooth, continuous, oxidation-free*

INTRODUCTION

Silver (Ag) is often employed for innovative applications, optical switching, optical amplification, optical modulation, plasmonics, microcavities, optical metamaterials, low-emissivity coatings, and many other applications in nanophotonics.[1−4] This is mainly due to its high electrical conductivity, low refractive index (~0.1 in the visible) and low loss at VIS-NIR optical frequencies. However, it is known that Ag films deposited by conventional techniques, including electron beam evaporation, chemical vapor deposition, electroless plating, and sputtering,[5−9] tend to grow on dielectrics or oxidized surfaces in island-like mode (Volmer−Weber growth mode)[10−13] and consequently exhibit a rough surface morphology with a large grain size and high resistivity,[14−16] which severely affect the performance of devices.

Therefore, it is of great importance for numerous practical applications to fabricate ultrasmooth Ag films with a subnanometer scale roughness, low resistivity, and a high degree of thickness uniformity. A recent work[17] has demonstrated that by a combination of template stripping and patterning on silicon substrates, a 30 nm thick thermally evaporated Ag film with 0.34 nm root-mean-square (RMS) roughness can be obtained. Further studies[18,19] showed that the use of transition metal seed layers also improves the quality of Ag surface morphology giving rise to a semitransparent, homogeneous, spike free, conductive and adherent layer, while Logeeswaran et al.[20] reported a simple method to create ultrasmooth Ag films by electron beam evaporation of a germanium (Ge) seed layer with a thickness of 0.5−15 nm atop of SiO_2/Si(100) substrates. A dramatic improvement of surface roughness down to about 0.6 nm (RMS) was achieved. Although deposition of Ge on silicon or oxidized substrates leads to a Volmer−Weber growth mode, the density of Ge nuclei was much larger and the islands were significantly smaller than those for Ag deposited directly on the substrate, allowing a very smooth and planar surface similar in smoothness to a layer-by-layer growth mode (Frank−Van der Merwe).[21,22]

In this paper, a sputtered 1 nm thick Cu seed layer is shown as an effective approach to produce atomically smooth Ag films with thicknesses less than 10 nm and greater electrical conductivity in comparison to monolayer Ag films. Copper is an inexpensive material with excellent electrical and optical properties and is already used widely in microelectronics industry. Because of its higher surface energy in comparison to Ag and Ge, it acts as a perfect seed layer for the growth of Ag films. Coalescence of Ag films induced by the seed layer leading to the formation of a continuous film with a percolation thickness as low as 3 nm has been achieved together with subnanometer surface roughness (RMS). A Cu seed layer also

Received: December 17, 2012
Accepted: March 20, 2013
Published: March 20, 2013

reduced the RMS roughness of Ag films, measured over a large area, leading to a concomitant factor of 2 reduction in the electrical resistivity when compared with previous reports on Ge/Ag films.[20] In addition, because of the lower percolation thickness, we were able to reduce the minimum thickness required to obtain a continuous Ag film down to 3 nm, which is substantially lower than that reported in literature for Ag films, thus paving a way for the deposition of smooth, ultrathin continuous Ag films. As a result of the improved uniformity, the oxidation of the Ag layer is strongly reduced to negligible values even after 4 months of exposure to ambient atmospheric conditions.

EXPERIMENTAL DETAILS

Fabrication. The films were fabricated on optically polished 1 mm thick UV grade fused silica substrates using a magnetron sputtering system (ATC Orion 8 HV) in an Ar atmosphere. The Cu and Ag layers were deposited sequentially without breaking the deposition chamber vacuum by DC sputter deposition from Cu and Ag targets of 3 in. diameter. The main chamber was typically evacuated to a base pressure below 1×10^{-7} Torr and deposition was performed under the following conditions: DC power 100 W, a pure Ar working pressure of 2×10^{-3} Torr and the target−substrate separation was 300 mm. The deposition rates, which are 25.6 Å/s for Ag and 15 Å/s for Cu, were determined using a MCM-160 quartz crystal and cross sectional SEM measurements of thick metal layers. Prior to the deposition, the substrates were ultrasonically cleaned with acetone and ethanol for 10 min, dried under flowing nitrogen, heated in oven at 100 °C for 30 min and finally transferred to the deposition chamber where they underwent a 15 min Ar plasma cleaning treatment at 40 W RF power and a pressure of 8×10^{-3} Torr. The depositions were performed at room temperature (22 °C) although a marginal increase of temperature (<4 °C) was observed due to the sputtering process.

Electrical Characterization. The electrical resistivity measurements of the deposited films were carried out by a Cascade Microtech 44//S2749 four-point probe system with a Keithley 2001 multimeter while transmittance and reflectance spectra were measured by a PerkinElmer Lambda 950 UV−vis−NIR spectrophotometer.

Surface Morphology Characterization. Surface morphology was investigated by a digital instrument D3100 Atomic Force Microscope (AFM) and FEI-Scanning Electron Microscopy (SEM). The AFM image analysis was carried out with Nanoscope 7.30 software.

$$\text{skewness} = \frac{1}{R_q^{\,3}}\frac{1}{N}\sum_{j=1}^{N} Z_j^{\,3}$$

Skewness measures the symmetry of surface data about a mean data profile. R_q is the RMS roughness. Skewness is a nondimensional quantity which is typically evaluated in terms of positive or negative. Where Skewness is zero, an even distribution of data around the mean data plane is suggested. Where Skewness is strongly nonzero, an asymmetric, one tailed distribution is suggested.

$$\text{kurtosis} = \frac{1}{R_q^{\,4}}\frac{1}{N}\sum_{j=1}^{N} Z_j^{\,4}$$

This is a nondimensional quantity used to evaluate the shape of data about a central mean. Graphically, it indicates whether data are arranged flatly or sharply about the mean.

Structural Characterization. Surface morphology was investigated by a digital instrument D3100 Atomic Force Microscope (AFM) and FEI-Scanning Electron Microscopy (SEM). The AFM image analysis was carried out with Nanoscope 7.30 software. High resolution X-ray reflectivity (XRR) and grazing incidence X-ray diffraction (GIXRD) measurements were performed using Cu Kα radiation and a Philips MRD goniometer equipped with a four-crystal Bartels Ge 220 monochromator. The Motofit code was used to fit the X-ray reflectivity data for scattering vectors greater than 0.15 Å^{-1}, which corresponds to incident angles where the X-ray beam's projection does not spill off the sample. The specular reflectivity is calculated using Parratts recursion formula (1954) for stratified thin films, as a function of the perpendicular momentum transfer. The Motofit reflectivity analysis module employs a genetic algorithm to simultaneously fit the real and imaginary parts of the scattering length densities, the film thickness and the interfacial roughness to all layers of a multilayer stack. The code was developed by Nelson[23] and is described in the reference.

RESULTS AND DISCUSSION

Several samples consisting of 6 nm thick Ag films with different seed layers, i.e. Si, Cu and Ti, were prepared under the same deposition conditions on double side polished UV grade fused silica substrates. The substrates had a very low RMS surface roughness; measured to be <5 Å. Figure 1 shows the two-dimensional AFM images for the following ultrathin film structures: 6 nm Ag, 1 nm Cu/6 nm Ag, 1 nm Si/6 nm Ag and 1 nm Ti/6 nm Ag samples, which respectively had a measured RMS surface roughness of 4.7, 0.4, 4.4, and 5.1 nm over a 10 μm × 10 μm area. As can be seen, the use of Cu as a seed layer led to exceptionally smooth Ag films with a RMS roughness less than 0.5 nm, thus reducing the roughness by a factor of 10 and suggesting a layer-by-layer growth mode. Table 1 summarizes

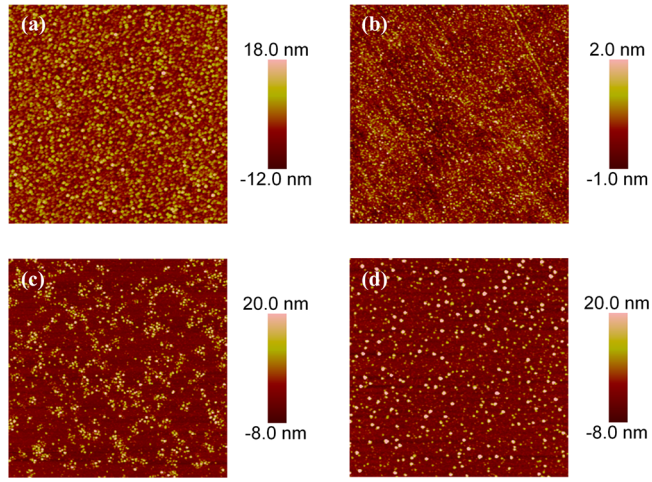

Figure 1. Two dimensional AFM images of (a) 6 nm Ag, (b) 1 nm Cu/6 nm Ag, (c) 1 nm Si/6 nm Ag, and (d) 1 nm Ti/6 nm Ag. The scanning area was 10 μm × 10 μm.

Table 1. Summary of Surface Morphology Parameters from AFM Image Analysis[a]

	RMS roughness (nm)	peak-to-valley roughness (nm)	image surface area difference (%)	resistivity (10^{-7} Ω m)
6 nm Ag	4.7	39.5	0.987	2.9
1 nm Cu/ 6 nm Ag	0.4	7.21	0.0144	0.80
1 nm Si/6 nm Ag	4.4	44.5	0.974	2.79
1 nm Ti/6 nm Ag	5.1	62.9	0.923	2.58

[a]The 3rd column quantifies the percentage increase of surface area of the real surface when compared to a flat surface of the same dimensions. A film with zero image surface area difference represents a perfect sample with zero surface roughness.

the different surface morphology parameters for the deposited films. The obtained RMS roughness is much lower than Ge/Ag films (0.6−0.8 nm) reported by Logeeswaran et al.[20] The 1 nm Cu seed layer forms energetically favorable nucleation sites for the incoming Ag atoms, thus leading to smoother films. The representative surface energies (γ) of Ag, Cu and SiO_2 are about 1.2−1.42, 1.96, and 0.26 J m^{2-}, respectively.[24,25] Because of its relatively high surface energy, the Cu seed layer produces a favorable wetting effect for the subsequent Ag growth.[26] Consequently, Ag films grown atop of a Cu seed layer tend to be smoother and exhibit a lower percolation threshold than Ag films grown directly on top of SiO_2, as is shown in the reported experiments. This phenomenon can also be explained in terms of bond dissociation energies (H, enthalpy) of Ag−Ag and Ag−Cu, which are H_{Ag-Ag} =162.9 ± 2.9 kJ mol^{-1} and H_{Ag-Cu} =176 kJ mol^{-1}, respectively.[27] The higher Ag−Cu bond energy (as compared to the Ag−Ag bond energy) indicates that the Ag atoms tend to be more tightly bound to the Cu surface than they are to their neighboring Ag atoms, which is a situation that is not prevalent in Ag−SiO_2 interfaces. Hence Ag islands on a Cu layer tend to be smoother than Ag films on SiO_2. The Si and Ti seed layers produced rougher Ag films indicating island growth mode where from a nucleation dot the film grows in three-dimensional islands till coalescence is reached. The histograms of surface−height values for 6 nm Ag and 1 nm Cu/6 nm Ag are shown in Figure 2. The Ag film with a 1 nm

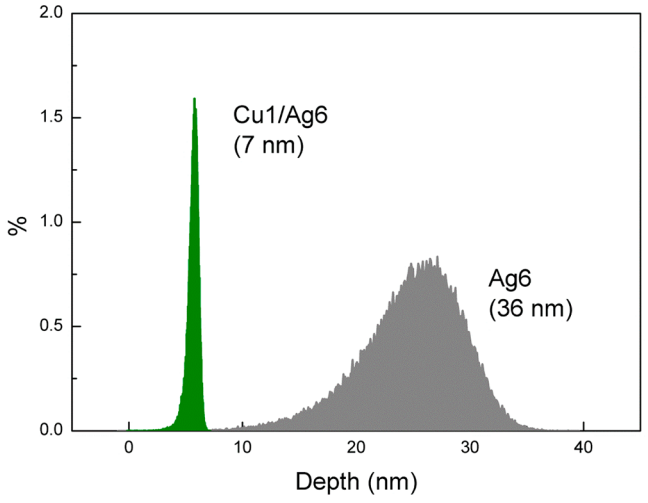

Figure 2. Histogram of the surface-height values for 6 nm Ag and 1 nm Cu/6 nm Ag. The peak-to-valley roughness is also shown for the coatings. The skewness and kurtosis corresponding to 6 nm Ag and 1 nm Cu/6 nm Ag films are −1.32, 7.26 and 0.65, 3.69 respectively.

Cu seed layer has a smoother surface compared with that of a single Ag film; the peak-to-valley height (R_Z) is of only ∼7 nm and it has a narrow and symmetric height distribution (skewness ≈ −1.32, kurtosis ≈ 7.26). The Ag film without any Cu seed layer is characterized by a more populated and broader distribution (skewness ≈ 0.65, kurtosis ≈ 3.69) with a total R_Z difference of ∼36 nm. The variation of surface morphology of Ag films with different seed layer thickness was also investigated. It has been observed that the minimum RMS roughness is achieved for a Cu seed layer thickness of 1 nm. Figure 3 shows the RMS roughness as a function of Cu seed layer thickness for a constant Ag thickness of 6 nm. An improvement in the RMS surface roughness from 4.7 to 0.7 nm

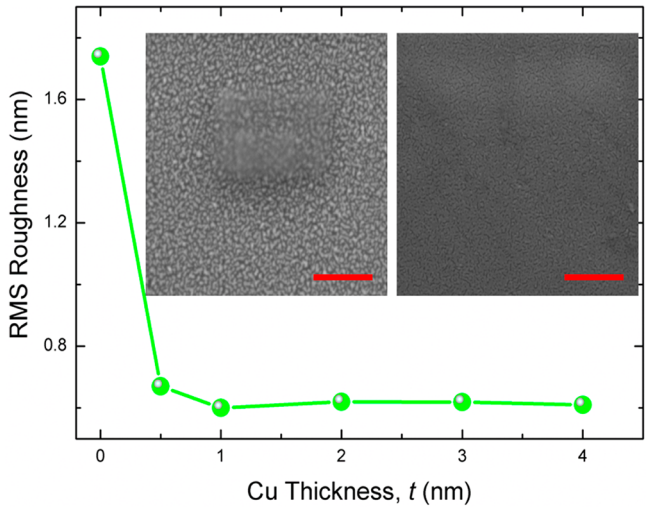

Figure 3. Variation of RMS roughness for 6 nm Ag film with seed layer thickness. For seed layer thicknesses greater than 4 nm the RMS roughness has roughly the same values of about 0.6 nm. The inset shows the SEM pictures without (left) and with a Cu seed layer (right). The scale bars are 500 nm.

was obtained for the first 0.5 nm of Cu deposited. For seed layer thicknesses greater than 1 nm the roughness remains the same at approximately 0.5 nm. The collected SEM surface micrographs of 6 nm thick Ag films with and without a 1 nm thick Cu layer are depicted in the inset of Figure 3. Without the Cu seed layer, the Ag film consists of metallic islands with an irregular shape and voids while denser and uniform planar morphology is observed in case of Ag film grown on Cu seed layer. The SEM images (inset Figure 3) provide further evidence of a discontinuous and coalescent structure together with a rough surface for the Ag film without any seed layer whereas the 1 nm Cu/6 nm Ag film is continuous with a homogeneous surface morphology due to a different growth mechanism altogether. This significant difference demonstrates the potential of the Cu seed layer for fabricating smooth Ag films.

In addition, high resolution X-ray reflectivity (XRR) measurements were acquired to confirm the smoothing effect of the Cu seed over a relatively large area. Figure 4 shows the experimental reflectivity curves for 6 nm Ag and 1 nm Cu/6 nm Ag samples. The oscillations in the reflected X-ray intensity showed sharper features, higher modulation, and were more pronounced in reciprocal space for the Cu/Ag structure in comparison with single Ag layer. The reflected X-ray intensity decreases more rapidly in reciprocal space for greater interfacial roughnesses, the interference fringes/oscillations present in the case of Cu/Ag structure clearly indicate much smoother films with lower surface and interface-roughness compared to a single Ag layer. A quantitative measurement of the film interface roughness was obtained by fitting thickness, the real and imaginary scattering length densities and interfacial roughness for all three layers of a slab model using genetic algorithm within the Motofit code.[23] The XRR analysis confirmed that the roughness, over an area of approximately 10 mm ×10 mm, was reduced by a factor of 2 when a Cu seeding layer was used to intermediate the Ag film.

Optical reflectance spectra of thin films are indicative of the wetting condition and mode of growth.[28,29] We investigated the influence of a Cu wetting layer on Ag growth through the

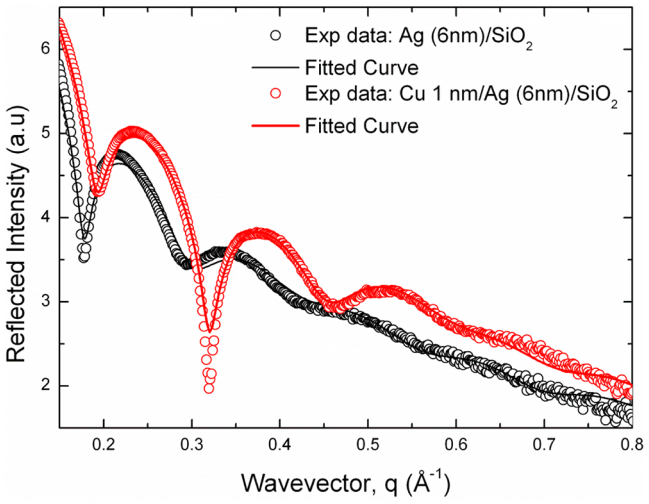

Figure 4. X-ray reflectivity (XRR) spectra for 6 nm Ag and 1 nm Cu/6 nm Ag films on silica substrates. The interference fringes/oscillations present in the case of Cu/Ag structure clearly indicates much smoother films with lower surface and interface-roughness.

reflectance spectrum in the 300−800 nm range. Figure 5 shows the reflectance spectra for Ag films of different thickness with

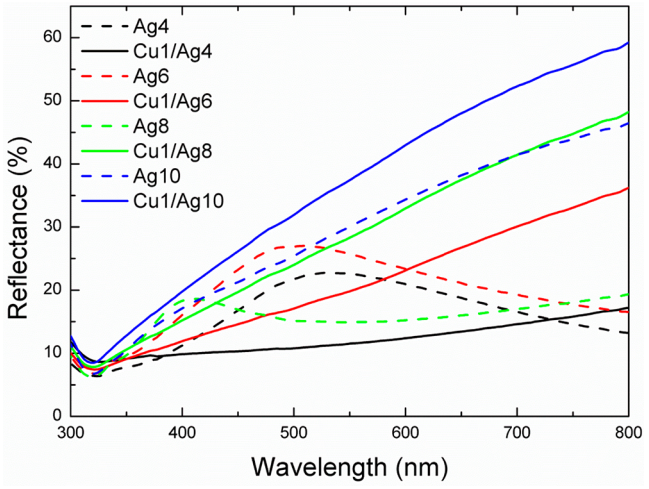

Figure 5. Comparison between the reflectance spectra of ultrathin Ag layers deposited with Cu 1 nm layer (continuous lines) and without seed layer (dashed lines). The localized plasmonic resonance behavior is clearly visible in the case films without the seed layer. The reflectance was measured at near-to-normal angle of incidence of about 15°.

and without Cu seed layer. As can be seen, the films without seed layer are characterized by a different trend with respect to the other set of samples having the additional seed layer. The peaks in the reflectance spectra shift to shorter wavelengths with increasing thickness; observed for films up to 8 nm Ag. This optical behavior is caused by a localized plasmon resonance in the metal particles.[30] The localized plasmon resonance in the earlier stages of film growth is induced by collective oscillations of conduction electrons, which are confined within the Ag grain.[31] This plasmon resonant character disappears when the nanostructuring of the Ag film disappears. This difference between the curves is due to changes in the morphology of the metal and indicates a discontinuous and a continuous Ag layer without and with Cu seed layer, respectively. From these measurements, it emerges that the 4 nm thick Ag film is already continuous on a Cu seed layer, while without the Cu seed layer a continuous film occurs at a higher thickness.

Once the optimum seed layer and thickness were determined, thin Ag films with a nominal thickness between 3 and 10 nm were sputtered with and without a 1 nm thick Cu seed layer. Four point probe electrical measurements, shown in Figure 6, reveal that when the thickness of the single layer Ag

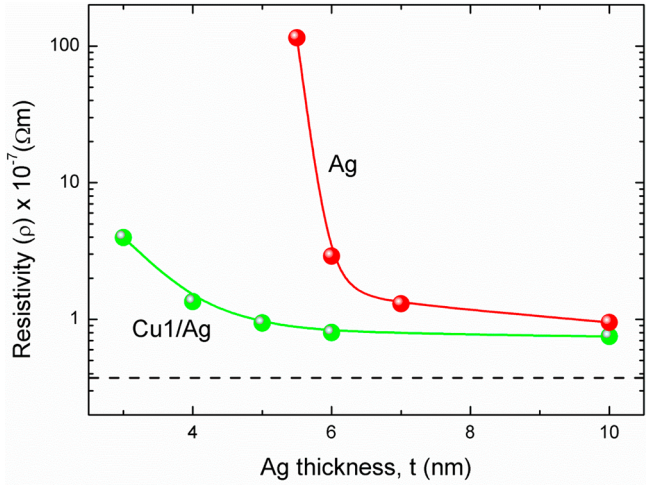

Figure 6. Comparison of electrical resistivity variation for Ag films with and without a Cu seed layer. The dashed line represents the resistivity of bulk Ag film of about 300 nm thickness deposited using the same sputtering process. Both types of films shown here approaches bulk behavior with thickness >100 nm.

film reaches a threshold value of 6 nm, a sharp drop in the electrical resistivity (ρ) by several orders of magnitude can be observed, indicating the coalescence of islands. In contrast, when a 1 nm thick Cu layer is used to aid the coalescence of the Ag film, the increase in electrical conductivity is less pronounced and the threshold thickness is much thinner. The results in Figure 6 demonstrate that the Ag film on a Cu seed layer exhibits a lower percolation threshold than a pure Ag film on silica substrates. By employing the Cu seed layer, the percolation thickness of Ag films was lowered to about 3−4 nm, which is much lower than the 11 nm percolation threshold of e-beam evaporated Ag films on Si/glass substrates reported elsewhere.[32] According to the scattering hypothesis based on the assumption of Matthiessen's rule, the resistivity (ρ) of a nonideal metal film can be expressed as

$$\rho = \rho_0 + \rho_{GB} + \rho_{SS} + \rho_{SR} \quad (1)$$

where the contributions of grain-boundary (ρ_{GB}), surface scattering (ρ_{SS}), and surface roughness (ρ_{SR}) are added to the bulk resistivity value ρ_0. Finzel and Wissmann[33] extensively studied the effect of surface roughness on the electrical resistivity of metal films and found that the roughness term in eq 1 varies proportional to inverse of third power of film thickness, that is, t^{-3}, which implies that the surface roughness plays a major role in ultrathin metal films when $t < l$, where l is the mean free path of the bulk metal. In our case, for example 6 nm Ag and 1 nm Cu/6 nm Ag having roughness 4.7 and 0.4 nm, the resistivity of the former was about 3.5 times of the later.

dx.doi.org/10.1021/am303147w | ACS Appl. Mater. Interfaces 2013, 5, 3048−3053

As evident from the roughness and resistivity values, the decrease in resistivity might also be attributed to improved crystallinity of the Ag film grown on the Cu seed layer. To validate this assumption grazing incidence X-ray diffraction GIXRD was measured for both sets of samples. The average grain size can be deduced by using Scherrer formula: $D = (0.9\lambda)/(B \cos \theta_B)$ where D is the grain size, B is the full width at half-maximum (fwhm), and θ_B is the Bragg angle. For the samples 6 nm Ag and 1 nm Cu/6 nm Ag the angular FWHMs calculated from the GIXRD experimental curves, shown in Figure 7, are 1.5° and 2.248°, respectively. Taking into account

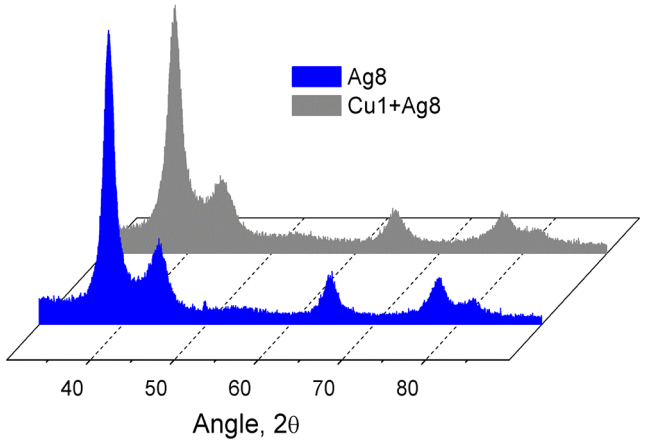

Figure 7. GIXRD spectra of 8 nm Ag films with and without seed layer. The *y*-axis represents the intensity in arbitrary units. The calculated grain size for the Ag films with seed layer was found to be 1.5 times smaller compared to Ag films without the seed layer.

those values from GIXRD spectra analysis the average grain size of the rough Ag film is 1.5 times larger than for the smooth film. Another advantage associated with the seed layer assisted growth of Ag films is that unlike the pure Ag film the Cu/Ag films offer much more resistance to corrosion in ambient conditions. This is because rougher Ag films present larger surface area to the O_2/H_2O present in the atmosphere leading to their oxidation within few hours after their preparation while the smoother Cu/Ag films remain stable even after 4 months of fabrication. Figure 8 shows the picture of 6 nm Ag film with (4 months after the deposition) and without Cu seed layer (24 h after deposition) stored in air ambient. For the pure Ag film, a change of color from gray to reddish-brown together with

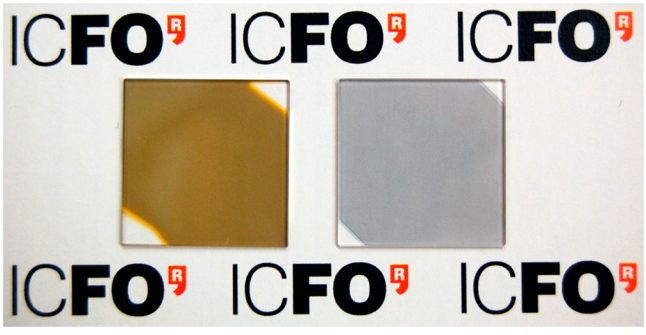

Figure 8. Pictures of 6 nm Ag film without (left) and with seed layer (right) 24 h and 4 months after deposition respectively. Freshly deposited Ag films without seed layer look exactly the same as the Ag film with seed layer 4 months after deposition as shown in the picture.

infinite electrical resistivity clearly indicates the oxidation of the sample. On the contrary, the Cu seeded Ag film showed the same electrical behavior over 4 month's period of time.

CONCLUSIONS

In this work, we found that adding a Cu seeding layer causes a significant decrease in the roughness of Ag films to subnanometer scales and reduces the minimum film thickness required to obtain a continuous layer, indicating an improved nucleation of the films deposited. It has been observed that a minimum Cu seed layer thickness of 0.5 nm is required to achieve atomically smooth and stable Ag films. Reflection spectroscopy measurements together with XRD and electrical resistivity measurements confirmed that the film with a Cu seed layer grows with layer-by-layer growth mode and a smaller grain size. Additional measurements showed that, the addition of the Cu seed layer reduces the percolation threshold of Ag by 3−4 nm. As a result of the improved uniformity, the oxidation of the Ag layer is strongly reduced to negligible values. Thus the Ag thin films described herein are well suited to various applications where ultrathin metallic films with low surface roughness are required. Such stringent demands are often prerequisites for nanoscale electronic and photonic applications.

AUTHOR INFORMATION

Corresponding Author

*E-mail: nadia.formica@icfo.es.

Author Contributions

⊥These authors contributed equally to this work.

Notes

The authors declare no competing financial interest.

ACKNOWLEDGMENTS

This work was supported by the Ministerio de Ciencia e Innovación through Grant TEC 2010-14832 and No.159224-1-2009-1-FR-ERA MUNDUS-EMJD. This research has also been supported by Obra Social "La Caixa".

REFERENCES

(1) Smith, D. R; Padilla, W. J.; Vier, D. C.; Nemat-Nasser, S. C.; Schultz, S. *Phys. Rev. Lett.* **2000**, *84*, 4184−4187.
(2) Shelby, R. A.; Smith, D. R.; Schultz, S. *Science* **2001**, *292*, 77−79.
(3) Fang, N.; Lee, H.; Sun, C.; Zhang, X. *Science* **2005**, *308*, 534−537.
(4) Yen, T. J.; Padilla, W. J.; Fang, N.; Vier, D. C.; Smith, D. R.; Pendry, J. B.; Basov, D. N.; Zhang, X. *Science* **2004**, *303*, 1494−1496.
(5) Yuan, H. K.; Chettiar, U. K.; Cai, W. S; Kildishev, A. V.; Boltasseva, A.; Drachev, V. P.; Shalaev, V. M. A *Opt. Express* **2007**, *15*, 1076−1083.
(6) Chi, Y.; Lay, E.; Chou, Y. I.; Song, Y.vH.; Carty, A. *Chem. Vap. Deposition* **2005**, *11*, 206−212.
(7) Jing, F.; Tong, H.; Kong, L.; Wang, C. *Appl. Phys. A: Mater. Sci. Process.* **2005**, *80*, 597−600.
(8) Yin, L. L.; Vlasko, V. K. V.; Pearson, J.; Hiller, J. M.; Hua, J.; Welp, U.; Brown, D. E.; Kimball, C. W. *Nano Lett.* **2005**, *5*, 1399−1402.
(9) Kapaklis, V.; Poulopoulos, P.; Karoutsos, V.; Manouras, Th.; Politis, C. *Thin Solid Films* **2006**, *510*, 138−142.
(10) Hu, M.; Noda, S.; Komiyama, H. *Surf. Sci.* **2002**, *513*, 530−538.
(11) Ohring, M. In *Materials Science of Thin Films*, 2nd ed.; Academic Press: San Diego, CA, 2002; Vol.*1*, p 386.
(12) Campbell, C. T. *Surf. Sci. Rep.* **1997**, *27*, 1−111.

(13) Kundu, S.; Hazra, S.; Banerjee, S.; Sanyal, M. K.; Mandal, S. K.; Chaudhuri, S.; Pal, A. K. *J . Phys. D: Appl. Phys.* **1998**, *31*, L73−L77.
(14) Marechal, N.; Quesnel, E.; Pauleau, Y. *J. Vac. Sci. Technol., A* **1994**, *12*, 707−713.
(15) Kim, H. C.; Theodore, N. D.; Alford, T. L. *J. Appl. Phys.* **2004**, *95*, 5180−5188.
(16) Islam, M. S.; Liz.; Chang, S. C.; Ohlberg, D. A. A.; Stewart, D. R.; Wang, S. Y.; Williams, R. S. In *Proceedings the th IEEE Conference on Nanotechnology*; IEEE: Nagoya, Japan, 2005; Vol. *80*, p 83.
(17) Nagpal, P.; Lindquist, N. C.; Oh, S. H.; Norris, D. J. *Science* **2009**, *325*, 594−597.
(18) Fukuda, K.; Lim, S. H. N.; Anders, A. *Thin Solid Films* **2008**, *516*, 4546−4552.
(19) Anders, A.; Byon, E.; Kim, D. H.; Fukuda, K.; Lim, S. H. N. *Solid State Commun.* **2006**, *140*, 225−229.
(20) Logeeswaran, V. J.; Kobayashi, N. P.; Islam, M. S.; Wu, W.; Chaturvedi, P.; Fang, N.; Wang, S. Y.; Williams, R. S. *Nano Lett.* **2009**, *9*, 178−182.
(21) Bauer, E. *Z. Kristallogr.—Cryst. Mater.* **1958**, *110*, 395−431.
(22) Bauer, E.; Van der Meme, J. H. *Phys. Rev. B.* **1986**, *33*, 3657−3671.
(23) Nelson, A. *J. Appl. Crystallogr.* **2006**, *39*, 273−276.
(24) Kendall, K. *J. Phys. D: Appl. Phys.* **1990**, *23*, 1329−1331.
(25) Jaccodine, R. J. *J. Electrochem. Soc.* **1963**, *110*, 524−527.
(26) Israelachvili, J. N. *Intermolecular and Surface Forces*; Academic Press: London, 1992; pp 196, 275, 280, 415.
(27) Lide, D. R.; In *C.R.C Handbook of Chemistry and Physics*, 87th ed.; CRC Press: Devon U.K, 2007; p 9−54.
(28) Heavens, O. S. *Rep. Prog. Phys.* **1960**, 23.
(29) Taneja, P.; Ayub, P.; Chandra, R. *Phys. Rev. B* **2002**, *65*, 245412.
(30) Bulíř, J.; Novotný, M.; Lynnykova, A.; Lančok, J. *J. Nanophotonics* **2011**, *5*, 1−10.
(31) Kreibig, U.; Vollmer, M. *Optical Properties of Metal Clusters*; Springer Series in Material Sciences; Springer-Verlag: Berlin, 1995; p 25.
(32) Nyga, P.; Drachev, V. P.; Thoreson, M. D.; Shalaev, V. M. *Appl. Phys. B: Laser Opt.* **2008**, *93*, 59−68.
(33) Hans,P. W.; Finzel, U. *Electrical Resistivity of Thin Metal Films*; Springer Tracts in Modern Physics; Springer-Verlag: Berlin, 2007; p 223.